(Received 17 June 2025, Accepted 24 July 2025, Scheduled 4 August 2025)

# Quadband Octagon Patch Antenna to Broadband MIMO Antenna Conversion by Using Defective Ground Structure

Katari Manjunath* and Sanam N. Reddy

*ECE Department, SV University College of Engineering, Tirupati, India*

**ABSTRACT:** In this paper, a Quadband Octagon Patch Antenna is designed whose operating frequencies are 20.22 GHz, 23.64 GHz, 27.35 GHz, 28 GHz, 28.37 GHz which achieved return losses of −19.67 dB, −19.14 dB, −19.66 dB, −19.04 dB, −19.04 dB, −20.41 dB and gain of 6.1 dB, respectively. The substrate employed in this antenna is FR4, which features a dielectric constant value 4.4 and a loss tangent value of 0.002. With a radiation efficiency of 90.85%. This antenna is small, measuring only $15 \times 25 \times 1.6\,\text{mm}^3$ dimensions. Multiple slots of different lengths are inserted in an antenna to form a 5G Quadband Octagon Patch Antenna in order to accommodate more operating frequencies. Later, a $2 * 2$ MIMO octagon patch antenna having a 3.6 mm radius, $50 \times 30 \times 1.6\,\text{mm}^3$ of dimensions, 4.4 dielectric constant, and 1.6 mm thickness with defective ground structure is designed. Here, this single quad-band antenna was turned to a broadband MIMO antenna by means of a defective ground structure.

## 1. INTRODUCTION

The Communication Industry from the year 2000 had recorded gigantic growth. During Pandemic, the utilization of mobile, laptop, and other communication devices has increased a lot. As time went on, the modern communication industry expanded from metropolitan areas to rural areas. Hence, a great demand for bandwidth and high speeds was created. Not even Fourth Generation (4G) speeds can satisfy everyone. So, every country is planning to migrate from 4G to 5G. The advent of 5G technology potentially revolutionized numerous industries, including the tech world. Improvements in smart highways, autonomous vehicles, high bandwidth augmented reality apps, IoT-enabled robotics, and sensors to boost customer service are all possible because of 5G technology's assurance of top-tier performance in the Internet of Things (IoT). High frequency 5G transmitting and receiving antennas, such as microstrip patch antennas, must be installed for accomplishing these speeds and enhanced bandwidth.

## 2. LITERATURE SURVEY

The Indian Department of Telecommunications (DoT) has identified many spectrums, including n71, n28, n5, n8, n3, n1, n40, and 23 GHz to 30 GHz, as 5G frequency bands [1]. An innovative wideband microstrip patch antenna with a nonuniform transmission line feed is presented employing nonlinear model predictive control (NMPC) [2]. An extensive analysis of the various antenna types, designs, and flexible antennas utilized in WBAN, together with a discussion of design concerns and comparisons, is presented in a study [3]. A recently constructed wideband monopole antenna with an f-form of radiating monopole and increased rear side is ideal for wideband applications [4]. A unique two-band monopole antenna featuring rectangular slots, elliptical half is demonstrated, which achieves significant two-band axial ratio and impedance bandwidth by the use of coplanar waveguide feeding [5]. There are various ways to boost the gain. Researches designed antennas by which the gain can be elevated by making a slot in the antenna patch [6, 7]. A microstrip antenna with a slotted rectangular and octagon patch has been developed to satisfy the growing need for 5G mobile communication services [8, 9]. For the 5G network, a 30 GHz square patch microstrip antenna with optimized voltage standing wave ratio (VSWR), greater gain, good bandwidth, and affordable radiation efficiency has been built [10]. Researchers created a prototype microstrip patch antenna which has the return loss of −18.30 dB at 4.6 GHz, using Ca0.05Zn0.95Al2O4 nanoparticles as the substrate material [11]. Researchers talked about four types of LI-slotted microstrip patch antennas [12], each with a distinct slot and varying gain, radiation efficiency, and bandwidth. They also explored wheel-shaped small wideband microstrip antennas [13]. Researchers proposed Tapered microstrip Patch Antenna (TMPA) with and without defected ground structure (DGS) [14], and two TMPAs are designed with defective ground by which gain is enhanced. In order to attain multiple bands, different slots of different shapes and sizes are chosen in the proposed paper.

## 3. ANTENNA DESIGN PROCEDURE

Formula (1) is used to determine the patch's radius in order to construct an elliptical cut octagon antenna [15].

$$r = \frac{F}{\left\{1 + \frac{2h}{\varepsilon_r \pi F}\left(\ln\left(\frac{\pi F}{2h}\right) + 1.7726\right)\right\}^{1/2}} \quad (1)$$

* Corresponding author: Katari Manjunath (kmanjunath4u@gmail.com).

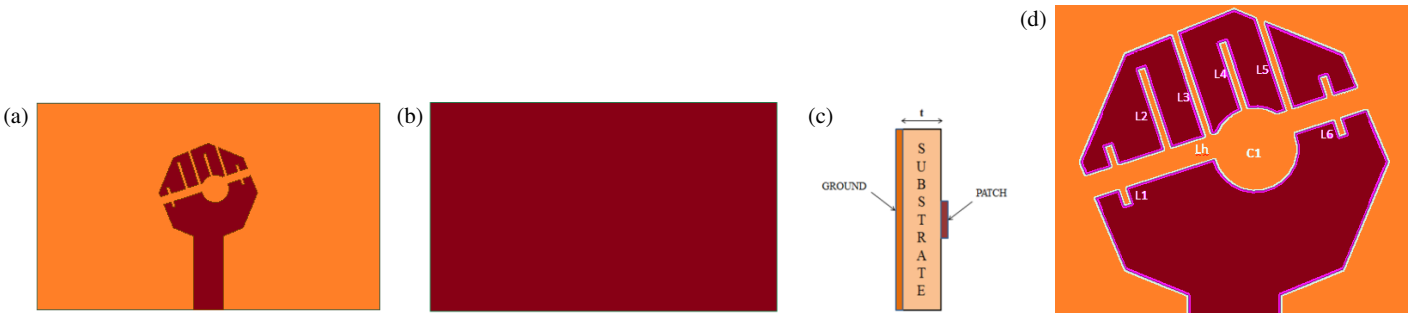


**FIGURE 1**. Quadband octagon patch antenna. (a) Upper view. (b) Rear view. (c) Side view. (d) Circular slot C1, Rectangular slots Lh, L1, L2, L3, L4, L5, L6.

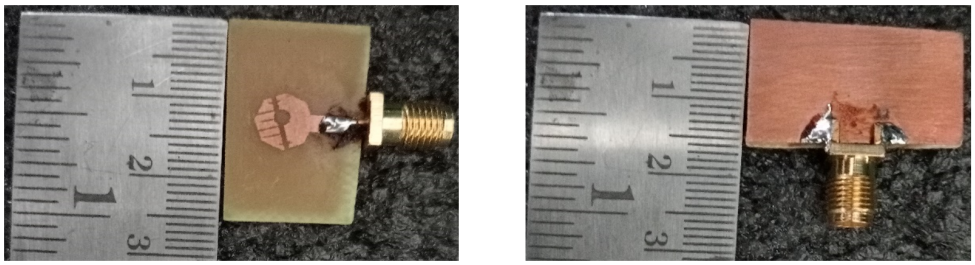

**FIGURE 2**. Fabricated quadband octagon patch antenna dimensions.

$$\text{where } F = \frac{8.791 * 10^9}{f_c\sqrt{\varepsilon_r}} \tag{2}$$

The fringing effect causes the patch to electrically enlarge. As a result, the effective patch radius is determined and provided by

$$r_e = r\left\{1 + \frac{2h}{\varepsilon_r \pi F}\left(\ln\left(\frac{\pi F}{2h}\right) + 1.7726\right)\right\}^{1/2} \tag{3}$$

Here, $r_e$ is the patch's effective radius; $\varepsilon_r$ and $h$ are dielectric constant and height for substrate; $f_r$ is the resonance frequency. The antenna's desirable center frequency for designing is $f_c = 26$ GHz. An FR4 substrate with a permeability of $\varepsilon_r = 4.4$ and a thickness of $t = 1.6$ in mm is used to build the suggested antenna. In the equations given above, these values are replaced. The operational frequency is 26.6 GHz, and the radius is 1.75 mm after the substitution. The purpose of conducting the parametric analysis for radius is to maximize gain. Results have been satisfactory with a radius 3.6 mm, so it is chosen.

## 4. ANTENNA GEOMETRY

### 4.1. 5G Quadband Octagon Patch Antenna

The dimensions of a monopole octagon patch antenna are $15 \times 25 \times 1.6\,\text{mm}^3$ with a radius of 3.6 mm. An FR4 substrate, featuring a 1.6 mm height and a 4.4 dielectric constant, is employed for creating a microstrip patch antenna between patch and ground. By applying High Frequency Structure Simulator (HFSS) parametric analysis, an octagon with a radius of 3.6 mm is picked. A 18° tilted horizontal rectangular slot $L_h$ is introduced at the center of the octagon whose length is 7 mm, and width is 0.6 mm. Similarly, 18° tilted vertical rectangular slots with lengths L1, L2, L3, L4, L5, L6 of 3 mm, 2.5 mm, two 2 mm, two 1.5 mm, and width of 0.2 mm are inserted into the octagon, respectively. Next, a circle of radius $c1 = 1$ mm is introduced at the center of Octagon. These rectangular slots and circle are then subtracted from Octagon. A 5G Quadband Octagon Patch Antenna is the end design.

This antenna in Figures 1 and 2 takes a number of specs from Table 1 into account while it is being designed. The antenna geometry is used to construct and simulate an octagon antenna with a single layer of elliptical cuts in HFSS.

**TABLE 1**. Single pole quadband antenna parameters.

| Parameters | Dimension (mm) |
|---|---|
| Ground Width ($W$) | 25 |
| Ground Length ($L$) | 15 |
| Thickness of Substrate ($t$) | 1.6 |
| Substrate's Dielectric constant | 4.4 |
| Width of Substrate ($W_s$) | 25 |
| Length of Substrate ($L_s$) | 15 |
| Radius of Octagon ($r$) | 3.6 mm |
| Feed Line Length ($L_f$) | 5.6 |
| Feed Line Width ($W_f$) | 3 |
| Slot Width | 1.41 mm |
| Slot Height | 0.2 mm |

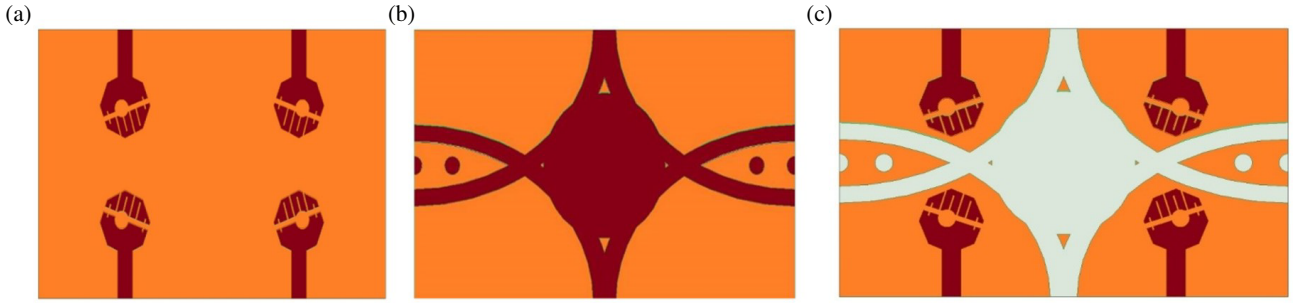


**FIGURE 3**. MIMO broadband octagon patch antenna. (a) Top view. (b) Back view. (c) Top view with top patch and bottom Ground.

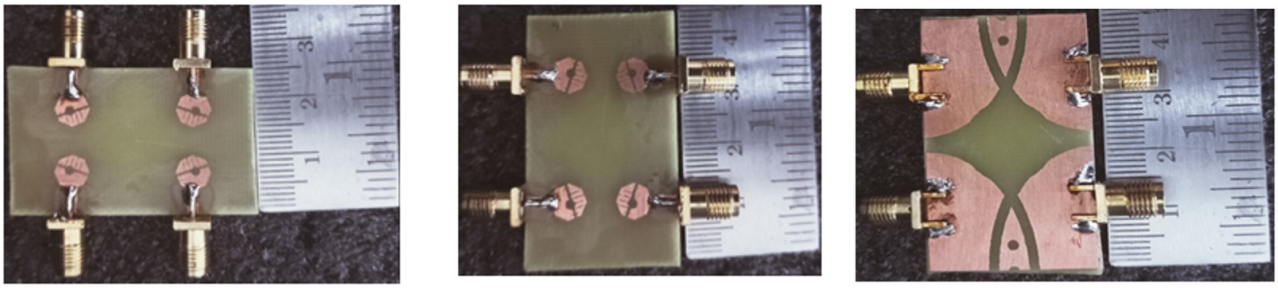

**FIGURE 4**. Fabricated broadband MIMO octagon patch antenna.

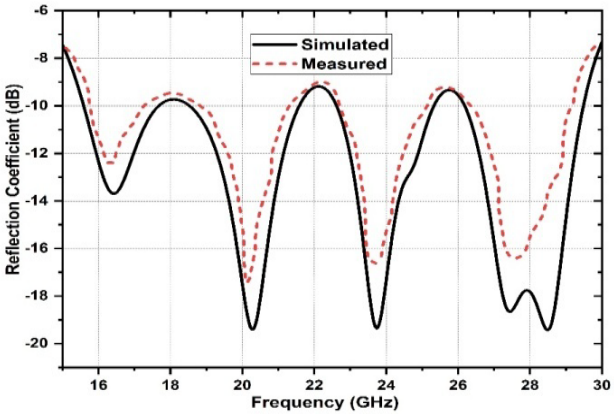


**FIGURE 5**. Quadband antenna's return loss.

### 4.2. 5G Broadband MIMO Octagon Patch Antenna

A 2∗2 multiple-input multiple-output (MIMO) octagon antenna has a 3.6 mm radius, $50 \times 30 \times 1.6\,\text{mm}^3$ dimensions, 4.4 dielectric constant, and 1.6 mm thickness. Further four Arcs of length 29.95 mm are inserted at each of the four corners in ground of microstrip patch antenna. Two circle slots of radius 1 mm and two half circles of radius 1.02 mm are inserted at two ends of ground. Hence, the ground becomes a defective ground structure. Finally, the resultant antenna is a $2 * 2$ MIMO Octagon Patch Antenna.

This MIMO antenna in Figure 3 takes a number of specs from Table 2 into account while it is being designed. Figure 4 shows the fabricated Broadband MIMO Octagon Patch Antenna. The antenna geometry is used to construct and simulate a MIMO octagon patch antenna with DGS in HFSS.

**TABLE 2**. MIMO broadband antenna parameters.

| Parameters | Dimension (mm) |
|---|---|
| Ground Width ($W$) | 50 |
| Ground Length ($L$) | 30 |
| Thickness of Substrate ($t$) | 1.6 |
| Substrate's Dielectric constant | 4.4 |
| Width of Substrate ($W_s$) | 50 |
| Length of Substrate ($L_s$) | 30 |
| Feed Line Length ($L_f$) | 5.6 |
| Feed Line Width ($W_f$) | 3 |
| Radius of Each Octagon ($r$) | 3.6 mm |
| Slot's Width | 1.41 mm |
| Slot's Height | 0.2 mm |
| Radius of circle in DGS | 5 mm |
| Arc length in DGS | 29.95 mm |
| Slot Radius | 1 mm |
| Half Slot Radius | 1.02 mm |

## 5. RESULTS AND DISCUSSION

### 5.1. 5G Quadband Octagon Patch Antenna

The Single Monopole Quadband Octagon Patch antenna achieved return loss of $-19.67$ dB, $-19.14$ dB, $-19.66$ dB, $-20.41$ dB, and gain of 6.1 dB, respectively. Radiation efficiency regarding this antenna reached 90.85%. Table 3 summarizes the results of the Quadband Octagon Patch Antenna's various parameters.

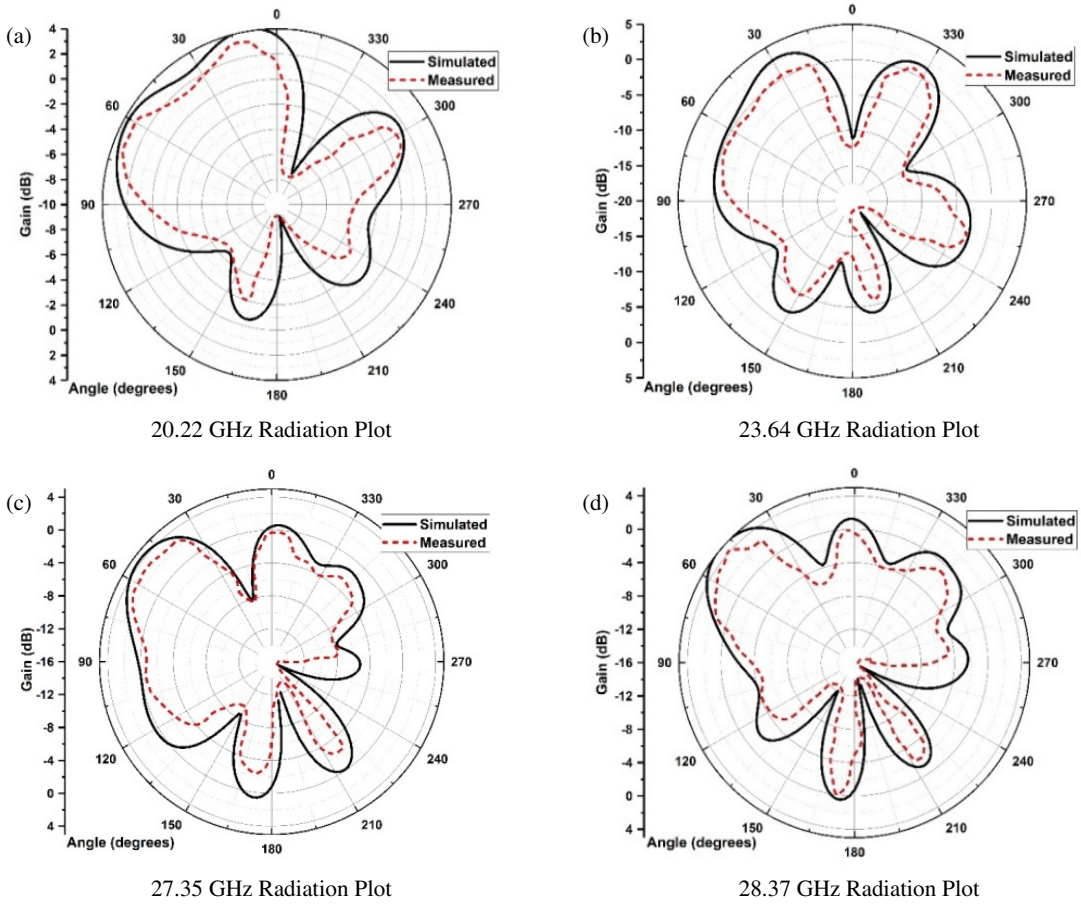


**FIGURE 6**. Quadband antenna's radiation plot.

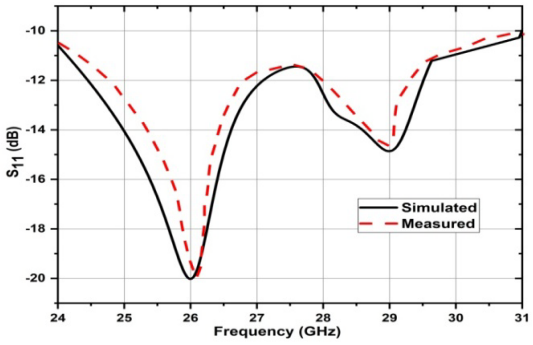


**FIGURE 7**. Broadband antenna's return loss.

**TABLE 3**. Quadband octagon antenna results.

| Parameters | Results |
|---|---|
| Frequency of operation | 20.22 GHz, 23.64 GHz, 27.35 GHz, 28.37 GHz |
| Bandwidth | 27.17 GHz–28.68 GHz (1.51 GHz) |
| Gain | 6.1 db |
| Radiation Efficiency | 90.85% |
| Front To Back Ratio | 19.29 |
| Return Loss | −19.67 dB, −19.14 dB, −19.66 dB, −20.41 dB |
| VSWR | 1.80, 1.92, 1.81, 1.66 |

**TABLE 4**. Broadband MIMO octagon antenna results.

| Parameters | Results |
|---|---|
| Frequency of operation | 24.7 GHz–30.20 GHz |
| Bandwidth | 5.5 GHz |
| Return Loss | −20.01 dB |
| Gain | 5.59 db |
| Front To Back Ratio | 21.29 |
| VSWR | Within 1–2 |
| Radiation Efficiency | 90.55% |

The Return Loss graph for the octagon antenna is displayed in Figure 5. Operating frequencies for this antenna include 20.22 GHz, 23.64 GHz, 27.35 GHz, 28 GHz, and 28.37 GHz with VSWR between 1 and 2. The Radiation Plots at 20.22 GHz, 23.64 GHz, 27.35 GHz, and 28.37 GHz are shown in Figure 6.

### 5.2. 5G Broadband MIMO Octagon Patch Antenna

The Broadband MIMO Octagon Patch antenna achieved the return loss of −20.01 dB and gain of 5.59 dB, respectively. The radiation efficiency of this antenna was 90.55%. Table 4 summarizes the outcomes of the Broadband MIMO Octagon Patch Antenna's various parameters.

Figures 7 and 8 show the graphs for this MIMO elliptical cut octagon patch antenna's return loss and radiation pattern. One

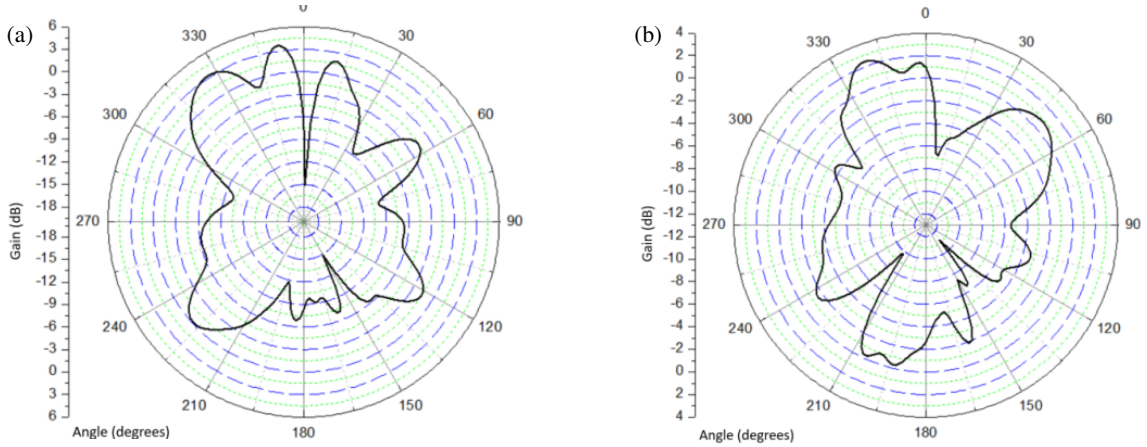


25.35 GHz Radiation Plot 29.11 GHz Radiation Plot

**FIGURE 8**. Broadband antenna's radiation plot.

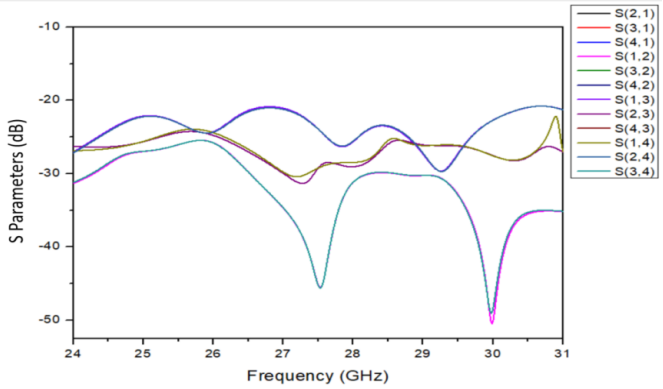


**FIGURE 9**. Broadband antenna's isolation plot.

crucial need of MIMO systems is the isolation among neighbouring antenna elements. To improve channel bandwidth and reduce radiation pattern deterioration, MIMO systems use a variety of antenna isolation strategies such as decoupling networks, parasitic elements, metamaterials, neutralisation lines, and electromagnetic bandgap structures. This proposed antenna uses isolation technique involves modifying the ground plane construction to create a band-stop effect, which effectively blocks the propagation of ground currents between the antenna components. Over the whole frequency range of operation, a 2-member MIMO antenna can achieve isolation levels of over 16 dB. An 8-element MIMO antenna is capable of achieving element-to-element isolation levels above 15 dB. If the massive MIMO antenna system is built using metamaterials, the observed isolation can reach 25 dB. A two- or three-element tiny multiple-input/multi-output (MIMO) antenna may reach isolation levels greater than 20 dB over its entire working frequency range. This suggested MIMO antenna may attain isolation levels of greater than 20 dB, as seen in Figure 9.

#### 5.2.1. Envelope Correlation Coefficient (ECC)

A diversity statistic called envelope correlation coefficient (ECC) gauges how closely adjacent MIMO antenna parts correlate with one another. Not only $S$-parameters, radiation patterns can be used to estimate it. Nonetheless, as it illustrates how various radiating elements among MIMO systems operate independently in their radiation pattern, the ECC value determined using the far field radiation pattern is strongly advised. Besides, most planar antennas are found to have loss; for this reason, one should steer clear of the method of calculating ECC using $S$-parameters. Equation (4) [16] provides a mathematical formula for ECC based on MIMO design radiation pattern data:

$$\mathrm{ECC}(k,m)=\rho_e(k,m,N)=\frac{\left|\sum_{n=1}^{N} S_{k,n}^{*} S_{m,j}\right|^2}{\left|\prod_{l=k\cdot m}\left(1-\sum_{n=1}^{N} S_{l,n}^{*} S_{n,l}\right)\right|}, \tag{4}$$

where $N$ represents all of the antenna components, and $i$ and $j$ are the port numbers. Enter $N = 4$ into the preceding calculation to determine the ECC between antenna components for a quad-port MIMO antenna. A value of ECC below 0.5 is considered acceptable for devices.

$$\begin{aligned}\mathrm{ECC}_{12} &= \rho_e(1,2,4)\\ &= \frac{\left|S_{11}^{*}S_{12}+S_{21}^{*}S_{22}+S_{13}^{*}S_{32}+S_{14}^{*}S_{42}\right|^2}{\left(1-|S_{11}|^2-|S_{21}|^2-|S_{31}|^2-|S_{41}|^2\right)\left(1-|S_{12}|^2-|S_{22}|^2-|S_{32}|^2-|S_{42}|^2\right)},\end{aligned} \tag{5}$$

where $\mathrm{ECC}_{12}$ represents the mutual coupling on port-1 brought upon by port-2. It is attainable to calculate $\mathrm{ECC}_{13}$, $\mathrm{ECC}_{14}$, $\mathrm{ECC}_{23}$, $\mathrm{ECC}_{24}$, and so on using Equation (5) [16]. Figure 10 shows the antenna's ECC value which is less than 0.5 as required.

#### 5.2.2. Diversity Gain (DG)

DG in wireless networks is a gauge of the robustness and quality of the MIMO antenna. As a result, within the permitted frequency range, the MIMO antenna's DG must be high, often

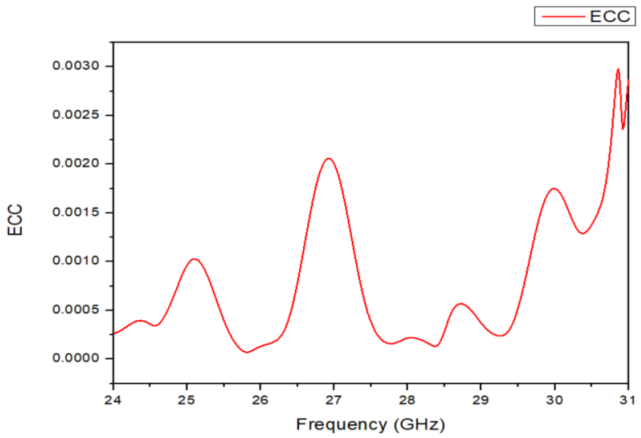


**FIGURE 10**. Broadband antenna's envelope correlation plot.

about 10 dB. To find the DG, we use the ECC value and plug it into Equation (6) [16]:

$$\mathrm{DG} = 10 \times \sqrt{1 - |\mathrm{ECC}_{qp}|^2} \tag{6}$$

Figure 11 illustrates the antenna's DG value, which is around 0.5 in accordance with specifications.

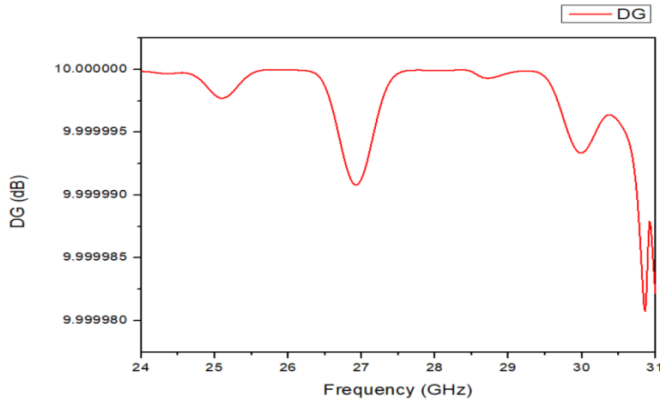


**FIGURE 11**. Broadband antenna's directivity gain.

### 5.2.3. Channel Capacity Loss (CCL)

The channel's capacity to carry data with nearly no loss is known as its channel capacity limit, or CCL. For any individual MIMO system, the prescribed CCL value is less than 0.4 bits/s/Hz. Equation (7) [16] provides the expression of CCL with $S$-parameters. The attained CCL value beneath 0.4 bits/s/Hz of this antenna is displayed in Figure 12.

$$C_{\mathrm{Loss}} = -\log_2 \det\left(\varphi^R\right) \tag{7}$$

$$\text{Where} \quad \varphi^R = \begin{bmatrix} \partial_{11} & \partial_{12} & \partial_{13} & \partial_{14} \\ \partial_{21} & \partial_{22} & \partial_{23} & \partial_{24} \\ \partial_{31} & \partial_{32} & \partial_{33} & \partial_{34} \\ \partial_{41} & \partial_{42} & \partial_{43} & \partial_{44} \end{bmatrix},$$

$$\partial_{ii} = (1 - |S_{ii}|^2 - |S_{ij}|^2),$$
$$\partial_{ii} = -(S_{ii}^* S_{ij} + S_{ji}^* S_{ij})$$
$$\text{for } i, j = 1, 2, 3, \text{ and } 4.$$

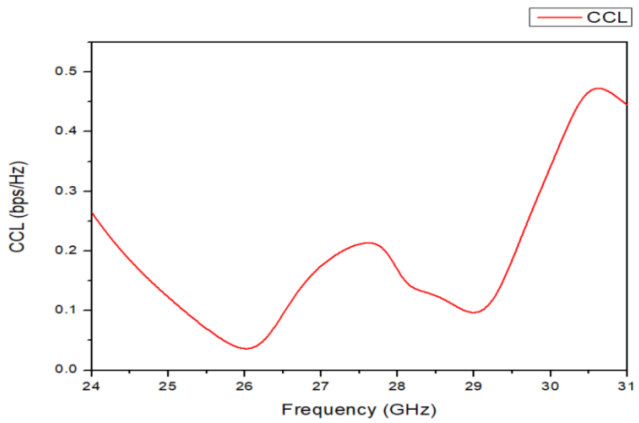


**FIGURE 12**. Broadband antenna's channel capacity loss.

### 5.2.4. Mean Effective Gain (MEG)

It is the received power ratio of the isotropic antenna divided by the received power of the MIMO antenna. As seen in Figure 13, the suggested antenna can achieve a ratio of $\mathrm{MEG}_j$ to $\mathrm{MEG}_i$ less than 3 dB, then a MIMO antenna which has the same power level will function better. Formulas (8) and (9) can be used to assess the MEG [17]:

$$\mathrm{MEG}_i = 0.5[1 - |S_{ii}|^2 - |S_{ij}|^2] \tag{8}$$
$$\mathrm{MEG}_j = 0.5[1 - |S_{ij}|^2 - |S_{jj}|^2] \tag{9}$$

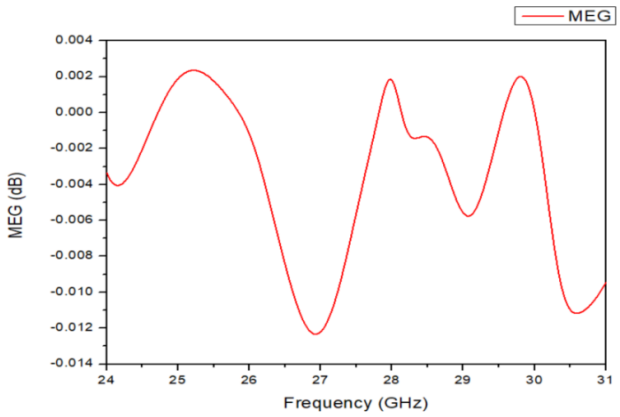


**FIGURE 13**. Broadband antenna's mean effective gain.

### 5.2.5. Total Active Reflection Coefficient (TARC)

The ratio of the patch's incidence power to the overall reflected power produced by the radiating elements in a multiple-input multiple-output (MIMO) system is called total reflected power, or TARC. For an N-port MIMO antenna, Equation (10) [17] may be employed to indicate the generalised TARC.

$$\mathrm{TARC} = \frac{\sqrt{\sum_{i=1}^{N} |b_i|^2}}{\sqrt{\sum_{i=1}^{N} |a_i|^2}} \tag{10}$$

Specifically, $b_i = [s] \cdot a_i$, where the scattering matrix's excitation vector and scattering vector are shown by the symbols $[s]$ and $[b]$, respectively.

**TABLE 5**. Comparative analysis of suggested antenna designs with earlier antennas.

| Antenna Model | Frequency (GHz) | $S_{11}$ (dB) | Voltage SWR | Bandwidth (GHz) | Gain (dB) | Efficiency % |
|---|---|---|---|---|---|---|
| Dual band hybrid directional resonator antenna [18] | 2.9–3.2 GHz, 4–4.6 GHz | −17.5 dB, −15 dB | Within 1–2 | 1 GHz | 4.5 dB | - |
| Eye bolt shape slotted patch antenna [19] | 28 GHz | −38 dB | 1.02 | 8 GHz | 5.5 dB | 87% |
| Circular patch antenna [20] | 632–1.142 GHz | −18 dB | Within 1–2 | 510 MHz | 5.5 dB | 85% |
| Reconfigurable key-shape antenna [21] | 1.9 GHz, 2.4 GHz, 3.1 GHz | 19.2 dB | Within 1–2 | 1.8–2.6 GHz | 2.5 dB | - |
| Bridged Circular Microstrip Patch Antenna [22] | 5, 7, 9, 11, 13, 14.55 (GHz) | −35 dB | Within 1–2 | 4.96–14.55 GHz | 4.81 dB | - |
| X-band microstrip patch antenna [23] | 8 to 12 GHz | −33 dB | −1.29 | 8.98 to 10.99 GHz | 5.68 dB | 90% |
| Proposed Single Quadband Antenna | 20.22 GHz, 23.64 GHz, 27.35 GHz, 28 GHz, 28.37 GHz | −19.67 dB, −19.14 dB, −19.66 dB, −19.04 dB, −20.41 dB | 1.80, 1.92, 1.81, 1.98, 1.66 | 1.51 GHz | 6.1 dB | 90.85% |
| Four Elements Reconfigurable MIMO [24] | 5.61–5.8 GHz | −28 dB | Within 1–2 | 0.2 GHz | 5.2 dB | 80% |
| Two Port Compact MIMO Antenna [25] | 2.43–2.50 GHz | −24.67 dB | Within 1–2 | 0.9 GHz | 4.68 dB | 58.53% |
| 12-Unit Asymmetric Mirror-Coupled Loop Antenna [26] | 3.3–3.6 GHz, 4.8–5.0 GHz | −24 dB | Within 1–2 | 0.3 GHz | - | 81% |
| Triple Band MIMO Antenna [27] | 3 GHz, 4.1 GHz, 5.2 GHz | −19.16 dB | Within 1–2 | 1 GHz | 4.29 dB | - |
| Dual-Band Four-Port Printed MIMO Antenna [28] | 3.1–3.6 GHz, 5.925–7.125 GHz | −20 dB | Within 1–2 | 1.5 GHz | 3.9 dB, 4.8 dB | 74% |
| Proposed MIMO Broadband Antenna | 24.7 GHz–30.20 GHz | −20.01 dB | Within 1–2 | 5.5 GHz | 5.59 dB | 90.55% |

Additionally, Equation (11) can be used to determine TARC for two-port MIMO antennas:

$$\text{TARC} = \frac{\sqrt{(|(S_{11} + S_{12}e^{j\theta})|^2 + |(S_{21} + S_{22}e^{j\theta})|^2)}}{\sqrt{2}} \quad (11)$$

It is expected that the antenna will absorb all of the power. Figure 14 illustrates that the optimal TARC value for a MIMO antenna is zero. When building a MIMO antenna, it is crucial to keep all of the antenna diversity parameters optimized within the previously mentioned limit.

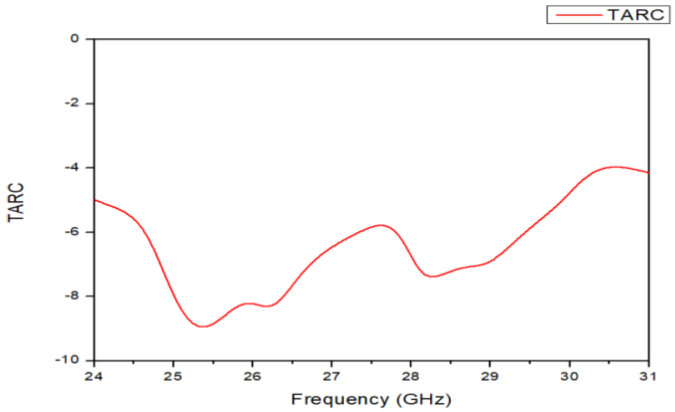


**FIGURE 14**. Broadband antenna's TARC.

## 6. COMPARISON WITH PROPOSED AND PREVIOUS ANTENNAS

As shown in Table 5, compared to all different patch antennas from references [18–23], the proposed Quadband antenna achieved greater gain of 6.1 dB and good radiation efficiency of 90.85%. There is a good blend of effectiveness, cost, and size in a microstrip antenna with a gain of 6.1 dB. It improves signal strength and directivity without making the design or size much more complicated or big. This makes it a good choice for situations where average performance is fine, and room is limited. The proposed quadband antenna provided an overall bandwidth of 1.51 GHz with four bands. Compared to all different MIMO patch antennas from references [24–28], the proposed MIMO broadband antenna achieved greater gain of 5.59 dB and good radiation efficiency of 90.55%. The proposed MIMO broadband antenna provided an overall bandwidth of 5.5 GHz with broadband. This 4-element MIMO antenna with a 5.5 GHz bandwidth and 5.5 dB gain is the best choice for next-generation wireless communication systems because it supports many novel and contemporary wireless standards and has a high

speed. Because of this, it works great for 5G, Wi-Fi 6E, and IoT networks that need high throughput, low delay, and smart spectrum use. The 90.85% transmission efficiency for quad-band antennas and 90.55% for MIMO antennas are very useful in the real world for 5G uses. Because of these high levels of efficiency, there will be more stable links, faster speeds, more data throughput, better range and coverage, especially in tough places or at higher frequencies (like mmWave). Minimizing the amount of power used means lower prices and better battery life for devices. Better user experience with steady connection, even in cities with lots of people can be met. Overall, these two high-efficiency antennas make 5G networks run smoothly, reliably, and cheaply. This makes them a key part of the next wave of wireless communication. One of the novelty and key contributions of the proposed MIMO antenna is its attained broadband capability with good gain which is not attained in previously existing antennas.

## 7. CONCLUSION & FUTURE SCOPE

This 5G Quadband Octagon Patch Antenna features a radiation efficiency of 90.85% and operates at frequencies of 20.22 GHz, 23.64 GHz, 27.35 GHz, 28 GHz, and 28.37 GHz. Its gain is 6.1 db, correspondingly. The total bandwidth of this antenna was 1.5 GHz. This 5G MIMO broadband octagon patch antenna features a radiation efficiency of 90.55%, an operational frequency range of 24.7 GHz–30.20 GHz, and a gain of 5.59 db. By using DGS, this single quad-band antenna was converted to broadband MIMO antenna. This antenna attained an overall bandwidth of 5.5 GHz. Applications involving mobile and fixed satellite communication, intersatellite communication, and intrasatellite communication are the ones for which this antenna is most beneficial. Applications for 5G are its primary use. In future, adding electronically steerable arrays and adaptive beamforming capabilities to the antenna could increase coverage, lower interference, and provide highly directional communication. Software-defined reconfigurable antennas could be developed in the future by including active components (such as PIN diodes, varactors, and Micro-Electromechanical Systems (MEMSs)) that allow for dynamic band switching or bandwidth tuning according to application requirements.

## REFERENCES

[1] Telecom regulatory authority of India. [Online]. Available: https://www.trai.gov.in/sites/default/files/Recommendations_11042022.pdf.

[2] Farahani, M. and S. Mohammad-Ali-Nezhad, "A novel wideband microstrip patch antenna with non-uniform feed based on model predictive," *Progress In Electromagnetics Research M*, Vol. 89, 101–109, 2020.

[3] Preethichandra, D. M. G., L. Piyathilaka, U. Izhar, R. Samarasinghe, and L. C. D. Silva, "Wireless body area networks and their applications — A review," *IEEE Access*, Vol. 11, 9202–9220, 2023.

[4] Andhe, K. K. and S. N. Reddy, "CPW-fed F-shaped compact monopole antenna with the dual-slot on the ground plane for WLAN and WiMAX applications," *Journal of Optoelectronics Laser*, Vol. 41, No. 11, 82–89, 2022.

[5] Andhe, K. K. and S. N. Reddy, "Dual-band circularly polarized compact planar dual slot monopole antenna," in *2021 International Conference on Recent Trends on Electronics, Information, Communication & Technology (RTEICT)*, 201–205, Bangalore, India, Oct. 2021.

[6] Modi, A., V. Sharma, and A. Rawat, "Design and analysis of multilayer patch antenna for IRNSS, GPS, Wi-Fi, satellite, and mobile networks communications," in *2021 12th International Conference on Computing Communication and Networking Technologies (ICCCNT)*, 1–6, Kharagpur, India, Jul. 2021.

[7] Mishra, R., R. Kalyan, and Y. M. Dubey, "Miniaturized W slot ultra wide band microstrip antenna for short distance communication," in *2017 International conference of Electronics, Communication and Aerospace Technology (ICECA)*, Vol. 2, 332–336, Coimbatore, India, Apr. 2017.

[8] Rayavaram, K., K. T. V. Reddy, and P. P. Kesari, "Compact UWB microstrip antenna with quadruple band-notched characteristics for short distance wireless tele-communication applications," *International Journal of Engineering & Technology*, Vol. 7, No. 1, 57–64, 2018.

[9] Manjunath, K. and S. N. Reddy, "Design and analysis of 5G broadband elliptical cut octagon patch antenna," *International Journal of Electrical and Electronics Research (IJEER)*, Vol. 12, No. 2, 647–653, 2024.

[10] Okwum, D., J. Abolarinwa, and O. Osanaiye, "A 30 GHz microstrip square patch antenna array for 5G network," in *2020 International Conference in Mathematics, Computer Engineering and Computer Science (ICMCECS)*, 1–5, Ayobo, Nigeria, 2020.

[11] Didde, S., R. S. Dubey, and S. K. Panda, "Prototype fabrication of microstrip patch antenna using ceramic nanoparticles," *Materials Today: Proceedings*, Vol. 89, 71–75, 2023.

[12] Nahas, M., "Design of a high-gain dual-band LI-slotted microstrip patch antenna for 5G mobile communication systems," *Journal of Radiation Research and Applied Sciences*, Vol. 15, No. 4, 100483, 2022.

[13] Kamal, S., M. F. B. Ain, U. Ullah, A. S. B. Mohammed, F. Najmi, R. Hussin, Z. A. Ahmad, M. F. B. M. Omar, M. F. A. Rahman, M. N. Mahmud, and M. Othman, "Wheel-shaped miniature assembly of circularly polarized wideband microstrip antenna for 5G mmWave terminals," *Alexandria Engineering Journal*, Vol. 60, No. 2, 2457–2470, 2021.

[14] Suvarna, K., N. Ramamurthy, and D. V. Vardhan, "Miniaturized and gain enhancement of tapered patch antenna using defected ground structure and metamaterial superstrate for GPS applications," *Progress In Electromagnetics Research C*, Vol. 108, 187–200, 2021.

[15] Balanis, C. A., *Antenna Theory: Analysis and Design*, 4th ed., John Wiley & Sons, 2016.

[16] Sengar, S., P. K. Malik, P. C. Srivastava, K. Srivastava, and A. Gehlot, "Performance analysis of MIMO antenna design with high isolation techniques for 5G wireless systems," *International Journal of Antennas and Propagation*, Vol. 2023, No. 1, 1566430, 2023.

[17] Sharma, P., R. N. Tiwari, P. Singh, P. Kumar, and B. K. Kanaujia, "MIMO antennas: Design approaches, techniques and applications," *Sensors*, Vol. 22, No. 20, 7813, Oct. 2022.

[18] Konch, R., S. Goswami, K. Sarmah, and K. K. Sarma, "Microstrip dual band hybrid directional resonator antenna with volume reduction," *AEU — International Journal of Electronics and Communications*, Vol. 171, 154889, 2023.

[19] Merin Joshiba, J. and D. Judson, "An eye bolt shape slotted microstrip patch antenna design utilizing a substrate-integrated

waveguide for 5G systems," *Automatika*, Vol. 64, No. 4, 943–955, 2023.

[20] Deshmukh, A. A., S. Surendran, A. Rane, Y. Bhasin, and V. A. P. Chavali, "Compact designs of circular microstrip antennas employing modified ground plane for wideband response," *AEU — International Journal of Electronics and Communications*, Vol. 176, 155130, 2024.

[21] Abdulhameed, A. A., F. M. Alnahwi, H. N. Al-Anbagi, Z. Kubík, and A. S. Abdullah, "Frequency reconfigurable key-shape antenna for LTE applications," *Australian Journal of Electrical and Electronics Engineering*, Vol. 20, No. 2, 138–146, 2023.

[22] Kurtulan, E., V. Mathur, P. Tyagi, and N. Singh, "Bridged circular microstrip patch antenna for wireless applications," *Materials Today: Proceedings*, Vol. 46, 5742–5747, 2021.

[23] Anand, S., "Planar polarization rotation reflective surface for X-band RCS reduction in microstrip patch antenna," *E-Prime — Advances in Electrical Engineering, Electronics and Energy*, Vol. 4, 100164, 2023.

[24] Choudhary, V., M. K. Meshram, and J. Hesselbarth, "Four elements reconfigurable MIMO antenna for dual band applications," *International Journal of Advances in Microwave Technology*, Vol. 7, No. 1, 274–282, 2022.

[25] Sharma, K. and G. P. Pandey, "Two port compact MIMO antenna for ISM band applications," *Progress In Electromagnetics Research C*, Vol. 100, 173–185, 2020.

[26] Ren, W., Z. Wang, W. Nie, W. Mu, C. Li, M. Wang, and W. You, "A 12-unit asymmetric mirror-coupled loop antenna for 5G smartphones," *Progress In Electromagnetics Research C*, Vol. 145, 141–152, 2024.

[27] Immadi, G., M. V. Narayana, A. Navya, A. S. Madhuri, B. V. Krishna, and M. V. S. Gopi, "Analysis of a triple band MIMO antenna for sub-6 GHz applications," *Progress In Electromagnetics Research B*, Vol. 107, 47–62, 2024.

[28] Rajagopalan, V., S. V. Sanu, and S. Rodrigues, "A dual-band four-port printed MIMO antenna with enhanced isolation and polarization diversity for midband 5G applications," *Progress In Electromagnetics Research Letters*, Vol. 121, 79–85, 2024.